ACS OMEGA

http://pubs.acs.org/journal/acsodf

Article

Naturally Occurring I81N Mutation in Human Cytochrome *c* Regulates Both Inherent Peroxidase Activity and Interactions with Neuroglobin

Yu Feng,[‖] Xi-Chun Liu,[‖] Lianzhi Li, Shu-Qin Gao, Ge-Bo Wen, and Ying-Wu Lin*

Cite This: *ACS Omega* 2022, 7, 11510−11518

Read Online

ACCESS | Metrics & More | Article Recommendations | Supporting Information

ABSTRACT: Human cytochrome *c* (*h*Cyt *c*) is a crucial heme protein and plays an indispensable role in energy conversion and intrinsic apoptosis pathways. The sequence and structure of Cyt *c* were evolutionarily conserved and only a few naturally occurring mutants were detected in humans. Among those variable sites, position 81 was proposed to act as a peroxidase switch in the initiation stages of apoptosis. In this study, we show that Ile81 not only suppresses the intrinsic peroxidase activity but also is essential for Cyt *c* to interact with neuroglobin (Ngb), a potential protein partner. The kinetic assays showed that the peroxidase activity of the naturally occurring variant I81N was enhanced up to threefold under pH 5. The local stability of the Ω-loop D (residues 70−85) in the I81N variant was decreased. Moreover, the Alphafold2 program predicted that Ile81 forms stable contact with human Ngb. Meanwhile, the Ile81 to Asn81 missense mutation abolishes the interaction interface, resulting in a ∼40-fold decrease in binding affinity. These observations provide an insight into the structure−function relationship of the conserved Ile81 in vertebrate Cyt *c*.

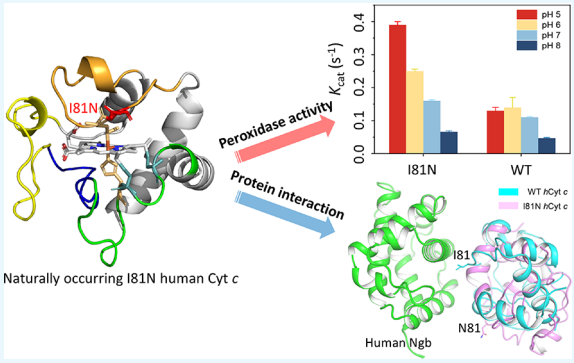

INTRODUCTION

Human cytochrome *c* (*h*Cyt *c*) is one member of a large distributed group of heme proteins, which contains a hexa-coordinated heme *c* with His18 and Met80 as axial ligands in the native state.[1−6] The porphyrin is covalently linked to the peptide chain via two thioether bonds through a conserved CXXCH motif. The protein is composed of five α-helices connected by several loop regions, namely Ω-loops (Figure 1, PDB code 3ZCF).[7] Cyt *c* is located on the outer surface of the inner mitochondrial membrane and has widely been known as an electron shuttle in the mitochondrial respiratory chain.[1] The electrons are transported from respiratory complex III to the terminal oxygen reductase via Cyt *c*, which is essential to cellular life throughout the electron−proton energy supplement process.

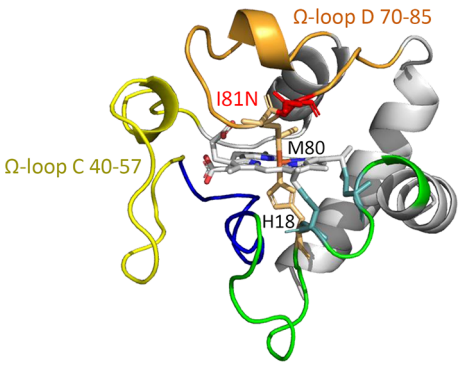

Figure 1. X-ray structure of *h*Cyt *c* (PDB code 3ZCF)[7] showing the overall structure, Ω-loops, and the heme coordination site. The mutation of I81N was modeled using PyMol.

Moreover, Cyt *c* has received interest for its multifunctionality involving the apoptosis pathway, gene regulation, and redox signaling.[1,4,5,8] The discovery of the pro-apoptosis activity of Cyt *c* was a breakthrough in the biological field. Cyt *c* can bind to apoptotic protease-activating factor 1 (apaf-1), which is essential for the successful assembly of an activated apoptosome. This process was related to the inherent peroxidase activity of Cyt *c*, which was further connected to missense mutation, post-translational modification, pH-dependent conformational change, and lipid binding.[9] In contrast to the inaccessible hexa-coordinated heme site in the native state, Cyt *c* can transform into alternative conformations under

Received: March 2, 2022
Accepted: March 14, 2022
Published: March 22, 2022

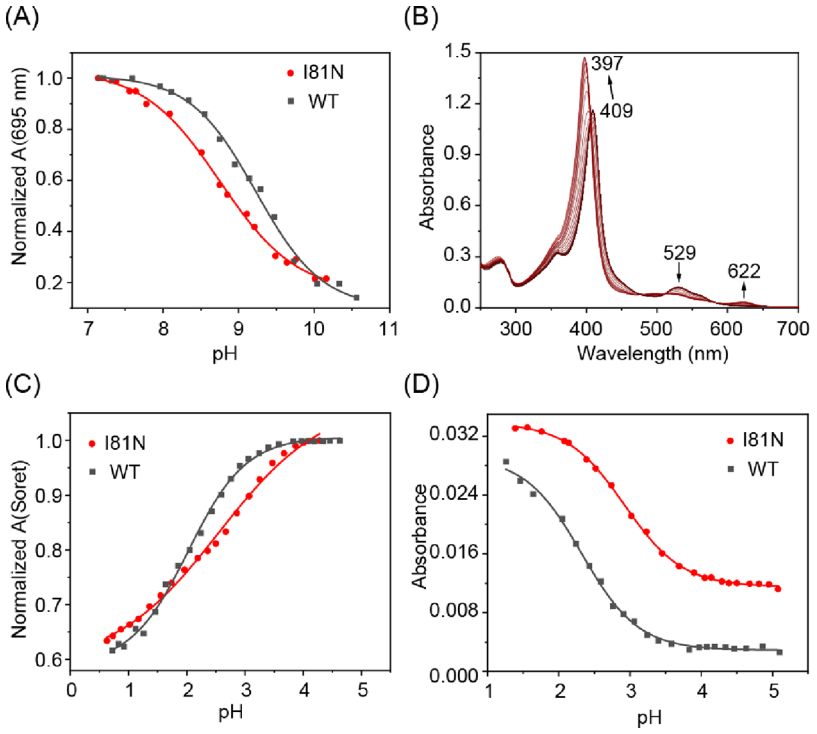

Figure 2. Alkaline conformational transition and acidic unfolding studies on the WT and I81N *h*Cyt *c*. (A) Normalized absorbance at 695 nm in the alkaline pH range. (B) pH-dependent UV−vis spectra changes of the I81N *h*Cyt *c* in acidic unfolding studies. (C) Normalized absorbance of the Soret band in the acidic pH range. (D) Absorbance at 622 nm in the acidic pH range.

these perturbations with a more accessible heme site and enhanced peroxidase activity. Thus, Cyt *c* can oxidize the lipids such as cardiolipin on the mitochondrial membrane to enhance the membrane permeability, which promotes the release of Cyt *c* to the cytoplasm and subsequently facilitates the assembly of the apoptosome.[10,11]

This view was supported by experimental results that can be classified as follows: (i) the modification of distal ligand Met80 or the structure change near Met80,[12−15] (ii) the structure changes aim to destroy the hydrogen bond networks constituted by Asn52, Tyr67, Thr78, and water,[16−18] (iii) the substitution of Lys relating to an alkaline conformation in different pH values,[19] and (iv) the losing of Met80 ligation and the formation of a well-defined pocket for binding hydrocarbons when Cyt *c* interacts with detergents,[20] a conformation rearrangement mimic for Cyt *c*-mediated cardiolipin oxidation.[21,22] *h*Cyt *c* was also found to interact with partner proteins to regulate the intrinsic apoptotic process. For example, Cyt *c* can bind to neuroglobin (Ngb), a heme protein highly expressed in the vertebrate nervous systems.[23] This interaction inhibits the binding between apaf-1 and *h*Cyt *c*, which was proposed as a crucial mechanism to protect mammalian neurons against the apoptotic stimulus.[24−26]

Because of the important and diverse functions of *h*Cyt *c*, a few naturally occurring variants were detected.[27] Although most of the 19 missense mutations are still lacking studies, 4 mutations (G41S, Y48H, A51V, and Lys100del) were found to be associated with autosomal dominant thrombocytopenia 4.[28−31] Our group also showed that the N52S variant exhibited a small fraction of high-spin species and 3−8-fold enhanced peroxidase activity at neutral pH.[18] Among other variants, we noticed that position 81 was only allowed a unique Ile-to-Asn missense mutation.[5] The appearance of the I81N *h*Cyt *c* variant inspired us to investigate the structural and functional consequences of the I81N substitution (Figure 1). Position 81 evolves from Ala in yeast to a conserved Ile residue in vertebrates.[11] Recently, Bowler and co-workers showed that the I81A mutation had a significant influence on the thermodynamics and kinetics of the access to alternate conformers of *h*Cyt *c*.[32] The substitution may perturb the heme environment close to distal ligand Met80 and Lys79/Lys72. Moreover, I81A *h*Cyt *c* exhibited a substantial enhancement in peroxidase activity, particularly below pH 7. In addition, Ile81 is suggested to interact with Lys67, Leu70, Val71, Ala74, Leu85, Tyr88, and heme of Ngb, whereas it lacks experimental studies.[26]

In this study, we combined experimental technologies and the protein structure prediction program Alphafold2[33,34] to investigate the properties of I81N *h*Cyt *c*, including the inherent peroxidase activity and the interaction with human Ngb (*h*Ngb). Notably, the results showed that I81N *h*Cyt *c* exhibited enhanced inherent peroxidase activity compared to that of wild-type (WT) protein, which was pH dependent and raised at low pH values. Moreover, it was found to interact much weakly with *h*Ngb, as determined by isothermal titration calorimetry (ITC), suggesting the unique role of Ile81 in supporting the structure and function of *h*Cyt *c* and its interaction with Ngb.

RESULTS AND DISCUSSION

Spectroscopic Studies of I81N hCyt *c*. The I81N *h*Cyt *c* variant was purified from *Escherichia coli* with high purity (Figure S1A) and was further confirmed by mass spectroscopy (Figure S1B). The ultraviolet−visible (UV−vis) spectra of the I81N variant were similar to those of the WT *h*Cyt *c* in both the ferric and ferrous forms (Figure S2), with similar maximum absorptions of the Soret band and Q bands. The circular

https://doi.org/10.1021/acsomega.2c01256
ACS Omega 2022, 7, 11510−11518

dichroism (CD) spectroscopy showed that the protein retained a typical α-helical structure with negative peaks at 208 and 222 nm and a positive peak at 190 nm in the far-UV region (Figure S3). Although the ellipticity (θ) value at 222 nm was slightly decreased compared to that of the WT *h*Cyt *c*, the proportion of the α-helical structure (~36%) and β-strand the structure (~10%) was almost the same for both proteins, as calculated by K2D2,[35] which suggests that the overall secondary structure was not perturbed by the I81N mutation.

To investigate whether the Ile-to-Asn mutation affects the local structural stability of Cyt *c*, we performed pH perturbation studies in both acidic and alkaline conditions. The Cyt *c* undergoes the acidic unfolding and the alkaline conformational transition process as described by Theorell and Åkesson.[36] These conformational transitions are related to the inherent peroxidase activities of Cyt *c* and are routinely performed to study the local structural dynamics around the heme moiety.[37] The specific peak of the Fe(III)−S bond at 695 nm was chosen to monitor the alkaline transition process, in which the Met-heme moiety transforms to a Lys-heme moiety.[38] It also induced a 7 nm blue shift at the Soret peak due to the structural change adjacent to the heme moiety (Figure S4). As shown in Figure 2A, the pH midpoint ($pH_{1/2}$) of the alkaline transition decreased from 9.23 ± 0.04 of the WT *h*Cyt *c* to 8.75 ± 0.03 of the I81N variant, with the proton linkage number (n) varying from 0.85 to 1 (Table 1). This result suggests that Ile-to-Asn substitution altered the Met80-heme ligation of *h*Cyt *c* in alkaline pHs.

Table 1. Experimental Parameters Related to the Local Structural Stability of I81N Cyt *c*

		I81N	WT
alkaline transition	$pH_{1/2\ 695nm}$	8.75 ± 0.03	9.23 ± 0.04
	n	0.85 ± 0.07	0.99 ± 0.08
acidic unfolding	$pH_{1/2\ soret}$	2.55 ± 0.07	2.03 ± 0.03
	n	0.48 ± 0.06	0.88 ± 0.05
	$pH_{1/2\ 622nm}$	2.92 ± 0.01	2.32 ± 0.03
	n	1.07 ± 0.03	1.09 ± 0.06
azide binding	k_{obs} (s^{-1})	0.0085 ± 0.002	0.0014 ± 0.0002

The alteration of the local structure of the I81N *h*Cyt *c* was also observed under acidic conditions. The acidic unfolding process was monitored at both the Soret band and the Q band at 622 nm (Figures 2B and S5). The Q band is contributed by the Fe(III)−O bond of the high spin H_2O-heme, as alternative conformers under acidic conditions.[39] The acid titration data show that the I81N variant exhibits a 0.5−0.6 units higher $pH_{1/2}$ than that of the WT protein (Figure 2C,D and Table 1). The $pH_{1/2\ soret}$ increases from 2.03 ± 0.03 to 2.55 ± 0.07 and the $pH_{1/2\ 622nm}$ increases from 2.32 ± 0.03 to 2.92 ± 0.01, respectively. Together with the alkaline titration data, the results show that the I81N variant unfolds for ~0.5 units of pH early in both acidic and alkaline conditions, which indicates that the Met80-heme moiety of the I81N variant might be less stable than that of the WT Cyt *c*.

To further confirm the lability of the Met80-heme ligation, we performed kinetic studies using a small ligand, the azide ion (N_3^-), to compete with the axial ligand Met80 in the protein matrix (Figures 3 and S6). The reaction is assumed to follow an SN_1 mechanism, in which the hexa-coordinated heme is in equilibrium with a penta-coordinated state and thus leaves an open proximal site for ligand binding (Figure 3C). The observed rate constant (k_{obs}) was obtained under pseudo first-order conditions. As shown in Table 1, I81N *h*Cyt *c* (k_{obs} = 8.53 ± 2.41 × 10^{-3} s^{-1}) reacts with azide ~6 times faster than the WT protein (k_{obs} = 1.44 ± 0.2 × 10^{-3} s^{-1}). The faster rate of the azide binding to the heme of I81N *h*Cyt *c* may suggest the faster dissociation of the Met80-heme ligation. Previous studies have shown that mutations in the Ω-loop D (70−85) such as K72A, P76C, K79G/M80X, I81A, F82K, and V83G may alter the heme crevice dynamics and ligand-binding properties.[19,32,40−42]

Peroxidase Activity of I81N hCyt *c*. The structural perturbations by I81N substitution may affect the inherent peroxidase activity of Cyt *c* because a tight and stable conformation is essential to keep it at a low peroxidase activity level in physiological conditions.[28] As recently reported, Cyt *c* samples the high-spin conformers more frequently under acidic conditions.[43] Meanwhile, the intermembrane space of mitochondria is an acidic pH environment (6.88 ± 0.09) and the intracellular pH decreases during apoptosis.[10,38,44] Thus, it is physiologically relevant to investigate the relationship between the peroxidase activity of I81N *h*Cyt *c* and the acidic pH change.

To confirm this speculation, we performed the stopped-flow assay under pH 5−8 conditions using guaiacol as a substrate (Figures 4 and S7). The kinetic parameters (k_{cat} and K_m) were obtained by fitting the data into the Michaelis−Menten model. As shown in Table 2, the difference in K_m was small for those of the WT and I81N Cyt *c* variant, which was comparable to the data of the I81A variant reported by Bowler and co-workers.[32] However, the k_{cat} value of the I81N variant exhibited a strong relationship with pH values, increasing from 0.16 s^{-1} at pH 7 to 0.39 s^{-1} at pH 5, whereas the difference was subtle in the case of the WT protein at pH 5−7 (Figure 4B). The enhancement of the peroxidase activity of I81N Cyt *c* suggests that the variant samples the high-spin conformation easier than the WT under acidic conditions, which agrees with the acidic unfolding experiments. Notably, the k_{cat} value for the I81N variant is also up to threefold higher than that of the WT at pH 5. The strong correlation between the peroxidase activity and acidic pH indicates that Ile81 is a peroxidase trigger in *h*Cyt *c*. It is worth mentioning that the peroxidase activity of the I81A variant (k_{cat} = 0.96 ± 0.01 s^{-1})[32] is 6-fold higher than that of the I81N (k_{cat} = 0.16 ± 0.01 s^{-1}) and 8.7-fold higher than that of the WT (k_{cat} = 0.11 ± 0.01 s^{-1}) at neutral pH, and thus the I81A mutation may not be allowed naturally.

In addition to the guaiacol assay, the heme degradation by H_2O_2 was also performed to gain more information about the enzymatic kinetics. The partial oxidation of Cyt *c* is a crucial step to initiating the peroxidase activity.[45] In the absence of a substrate, the activation of H_2O_2 in the heme center results in heme degradation by self-oxidation. This process was monitored at the Soret band, which decreased over time during the degradation process (Figures 5 and S8). The observed rate constants (k_{obs}) were obtained at various concentrations of H_2O_2. It showed the I81N variant degraded about 1.5−3-fold faster than the WT protein depending on the concentration of H_2O_2 (Figure 5B). It should be noted that the reaction between I81N Cyt *c* and H_2O_2 did not follow a pseudo first-order mechanism, with a positive intercept (~0.005 s^{-1}) representing the dissociation rate constant (k_d) of the Cyt *c*−H_2O_2 complex.[46] This observation is similar to those reported for H_2O_2 binding to other heme proteins such

https://doi.org/10.1021/acsomega.2c01256
ACS Omega 2022, 7, 11510−11518

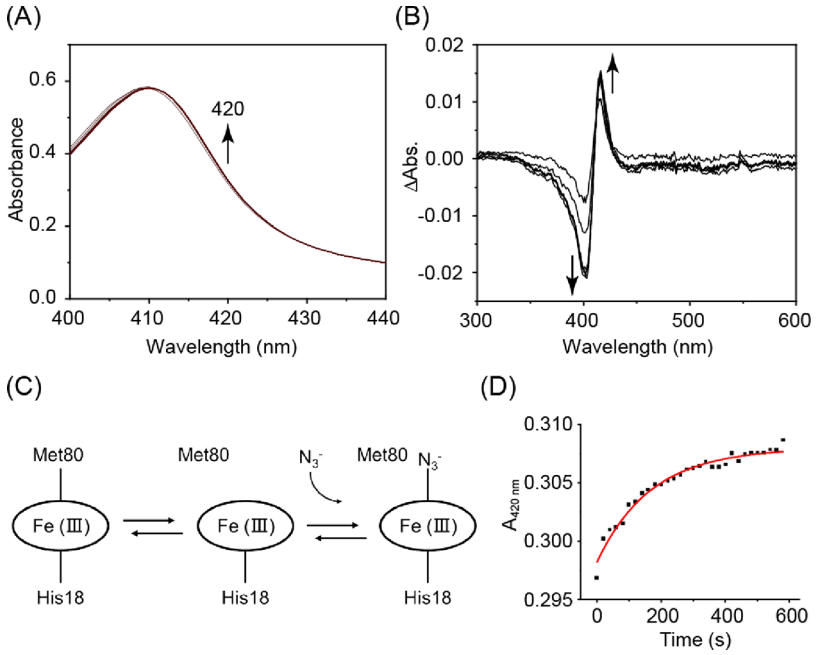

Figure 3. Azide-binding studies on I81N *h*Cyt *c*. (A) Time-dependent UV−vis spectra upon mixing 200 mM NaN_3 with 10 mM protein sample in 50 mM potassium phosphate buffer at pH 7.0, 25 °C. (B) Difference spectra obtained by subtracting the spectrum at 0 s. (C) Proposed SN_1 mechanism for the azide-binding reaction. (D) Absorbance changes at 420 nm upon NaN_3 titration.

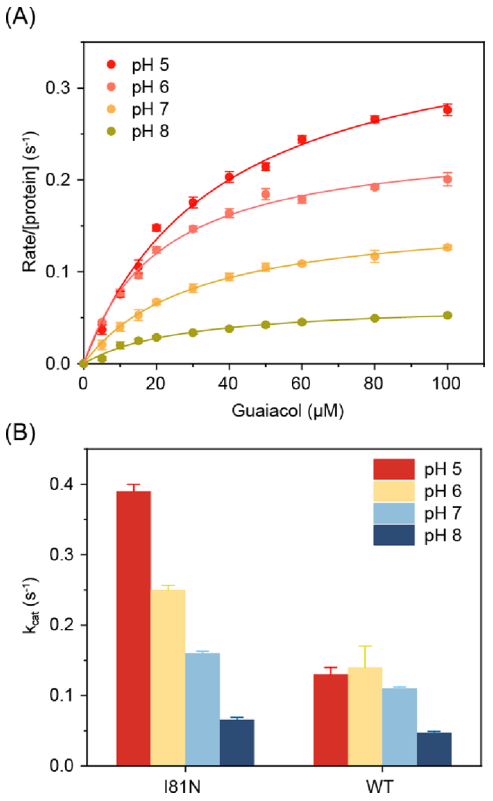

Figure 4. Peroxidase activity assay using guaiacol as a substrate. (A) Michaelis−Menten plots vs the concentrations of guaiacol for I81N *h*Cyt *c* at pH 5−8. (B) k_{cat} vs pH values for I81N and WT *h*Cyt *c*. The error bars are based on the standard deviation of six independent experiments.

as bacterial peroxidase and myoglobin mutants with altered heme active sites,[47,48] which suggests that the I81N mutation

Table 2. Kinetic Parameters of the Peroxidase Activity of *h*Cyt *c* Variants at Different pH Values with Guaiacol as a Substrate

	k_{cat} (s^{-1})		K_m (μM)	
pH	I81N	WT	I81N	WT
5.0	0.39 ± 0.01	0.13 ± 0.01	36.9 ± 3	50.2 ± 9
6.0	0.25 ± 0.006	0.14 ± 0.03	21.2 ± 2	20.0 ± 1
7.0	0.16 ± 0.003	0.11 ± 0.002	30.5 ± 1	27.5 ± 1
8.0	0.066 ± 0.003	0.047 ± 0.002	28.1 ± 3	12.9 ± 3

facilitates not only H_2O_2 activation but also its dissociation from the heme center.

Interactions between I81N hCyt *c* and Ngb. It is believed that the enhanced peroxidase activity of Cyt *c* is related to the instinct apoptosis pathway. However, it must be strictly regulated, especially in neurons. The interaction between Ngb and Cyt *c* was proposed as a crucial mechanism to protect neurons in vertebrates.[24] Previous ITC studies showed the dissociation constant between *h*Ngb and horse heart Cyt *c* was K_d = 22.0 ± 1.7 μM in 10 mM phosphate buffer.[49] Several acidic residues in Ngb were also found to participate in the interaction with Cyt *c*.[26,49−51] Meanwhile, depicting the precise binding interface is still a great challenge.

To gain more insight into the structure−function relationship of the conserved Ile81, we applied the most accurate protein structure prediction program Alphafold2 to predict the potential interactions between *h*Ngb and *h*Cyt *c*. The five WT *h*Ngb−*h*Cyt *c* models generated using Alphafold2 displayed a convergent interaction interface with a high predicted local distance difference test (pLDDT) score and a low predicted align error (Figures 6A,B). As the program identified, the interface hotspots include four pairs of hydrogen bonds (K72-D73, K86-D63, Q16-S91, and Q16-K95, Figure 6C) and several hydrophobic contacts (Figure 6D). Notably, the Ile81 forms a hydrophobic core, which interacts with the strictly

https://doi.org/10.1021/acsomega.2c01256
ACS Omega 2022, 7, 11510−11518

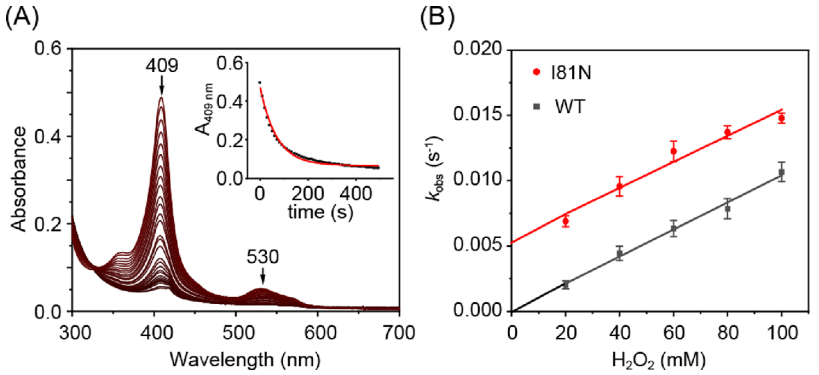

Figure 5. Heme degradation of *h*Cyt *c* by H_2O_2. (A) Time-dependent UV−vis spectra of I81N *h*Cyt *c* in a reaction with 100 mM H_2O_2. The spectral change of the Soret band was shown as an inset. (B) Linear fitting of k_{obs} as a function of H_2O_2 concentrations.

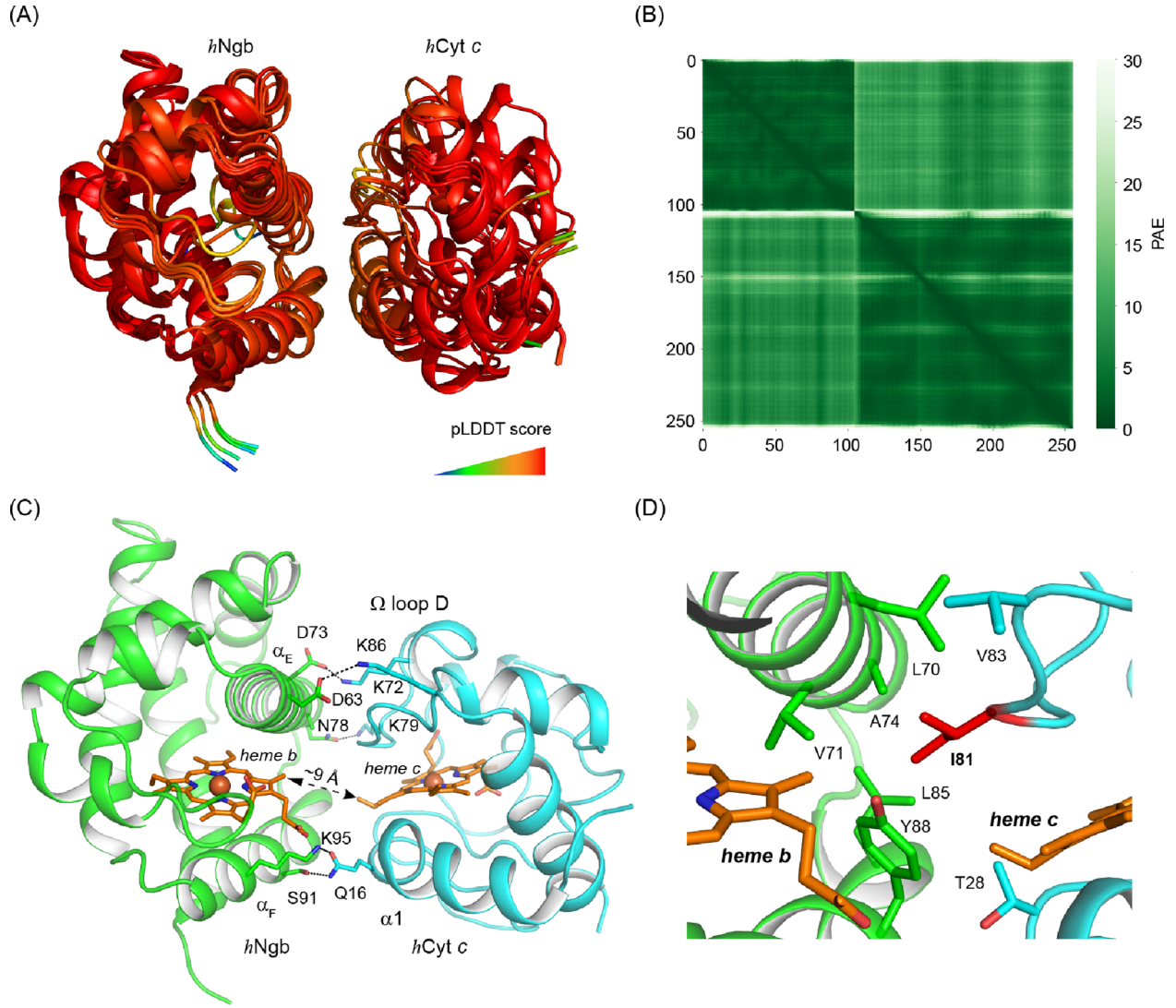

Figure 6. WT *h*Ngb−*h*Cyt *c* protein complex model predicted by the Alphafold2 multimer. (A) Cartoon representation of the five predicted models. These models were colored according to the pLDDT score. (B) Predicted alignment error of the model with the highest confidence. (C) Hydrogen bond networks in the predicted protein−protein interaction interface formed by the α_E and α_F helices of *h*Ngb (green) and the Ω loop D and the α1 helix of *h*Cyt *c* (cyan). The distance between the heme *b* and heme *c* groups was indicated as black dash arrows. (D) Hydrophobic core of the interaction interface. The Ile81 of *h*Cyt *c* was colored red.

conserved residues Leu70, Val71, Ala74, Lys85, and Tyr88 in Ngb (Figure S9). This is a reasonable prediction because these two proteins are coevolutionary in vertebrates and the Ile81 is conserved among vertebrate Cyt *c*. Other interface hotspots in *h*Cyt *c* include Gln16, Thr28, Lys72, Lys79, Val83, and Lys86 in both oxidation states (Figure S10). It should be noted that

https://doi.org/10.1021/acsomega.2c01256
ACS Omega 2022, 7, 11510−11518

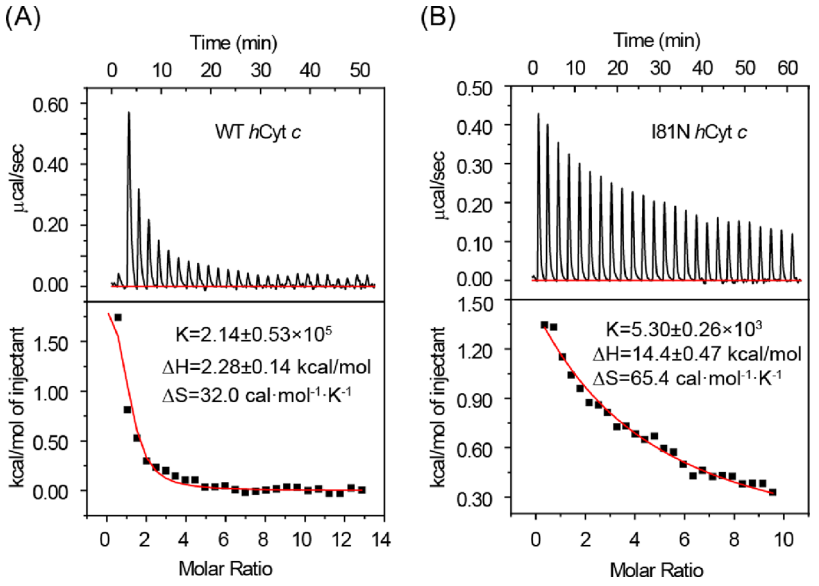

Figure 7. Representative ITC thermogram of WT (A) and I81N (B) *h*Cyt *c* titrated into *h*Ngb. Both samples were prepared in a 1 mM potassium phosphate solution at pH 7.0. The data were fitted to the OneSites binding model.

some of these residues are also located at the contacting interface with apaf-1, such as Ile81, Lys72, and Lys86 (Figure S11),[52] which suggests that the interaction between *h*Cyt *c* and apaf-1 might be blocked by the binding of Ngb.

To confirm that the Ile81 residue of *h*Cyt *c* plays a critical role in interaction with *h*Ngb, we performed ITC studies. To make a comparison of the binding affinity, we performed the titrations in 1 mM potassium phosphate solution at pH 7 (Figure 7) because the binding affinity was lower with the increase in the concentration of phosphate (Figure S12). The binding constant was determined to be $K_a = (5.30 \pm 0.26) \times 10^3$ M^{-1} (K_d = 189 μM) for I81N *h*Cyt *c* (the error was produced from the data fitting), which decreases almost 40-folds compared to that for the WT *h*Cyt *c*, $K_a = (2.14 \pm 0.53) \times 10^5$ M^{-1} (K_d = 4.67 μM). Moreover, the reaction enthalpy (ΔH) and entropy (ΔS) changes for I81N *h*Cyt *c* binding to Ngb were ~6-fold and ~2-fold higher than that of *h*Cyt *c*, respectively. The positive ΔH and ΔS suggest a predominant entropy-driven formation of the Cyt *c*−Ngb complex, resulting in negative Gibbs free energy (ΔG). The increased entropy may be related to the release of water molecules from the binding interface during the formation of the protein−protein complex.[49]

The Alphafold2 program suggests that the binding interface mediated by position 81 was abolished due to the Ile-to-Asn mutation in the hydrophobic core, resulting in different orientations for residue 81 (Figure 8A). The new contact interface includes Lys8, Ile11, Met12, Lys13, and Gln16 in I81N *h*Cyt *c* and Asp73, Leu70, Ala74, Leu85, Tyr88, and Ser91 in Ngb, where two hydrogen bonds (Q16-S91 and K8-D73) were formed in addition to hydrophobic interactions among other residues (Figure 8B). The molecular dynamics simulations further suggest that this interaction is less stable than that of the WT protein, with a large root-mean-square deviation (rmsd) (~6.5 Å) of the protein backbone (Figure S13). These experimental and simulation results thus confirm that the residue Ile81 is important for *h*Cyt *c* to interact with *h*Ngb.

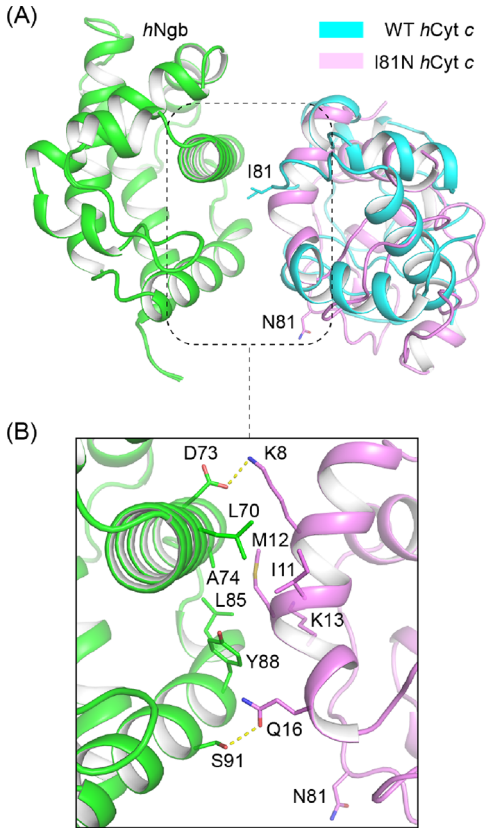

Figure 8. Complex models of *h*Ngb-WT/I81N *h*Cyt *c* predicted using Alphafold2. (A) Structural alignment of WT and I81N *h*Cyt *c*, showing the different orientations of residue 81. (B) Protein−protein interface of *h*Ngb-I81N *h*Cyt *c* in the model with the highest confidence.

CONCLUSIONS

In summary, we have shown that the naturally occurring I81N mutation in *h*Cyt *c* regulates both the inherent peroxidase activity and the interaction with human Ngb. The Ile-to-Asn mutation perturbs the local structural stability under both

https://doi.org/10.1021/acsomega.2c01256
ACS Omega 2022, 7, 11510−11518

alkaline and acidic pH conditions. The Met80-Fe(III) bond reacts with azide sixfold faster than that of the WT protein, which confirms the lability of Met80-heme ligation in the I81N variant. Therefore, the inherent peroxide activity was increased due to a more accessible penta-coordinated heme site. High-accuracy structure prediction by deep neural networks, the Alphafold2 program, suggests that Ile81 is located at the *h*Ngb−*h*Cyt *c* interaction interface, serving as the hydrophobic core. The mutation of the hydrophobic Ile to the hydrophilic Asn may abolish the specific interaction between *h*Cyt *c* and *h*Ngb. As further shown by the ITC studies, the apparent binding affinity decreased by ∼40-fold upon I81N mutation. Taken together, these results illustrate that the residue Ile81 of *h*Cyt *c* plays a critical role in protein function regulation, which provides an insight into the coevolution of Cyt *c* and Ngb in vertebrates.

■ ASSOCIATED CONTENT

Supporting Information

The Supporting Information is available free of charge at https://pubs.acs.org/doi/10.1021/acsomega.2c01256.

Materials and methods; SDS-PAGE of the purified WT and I81N Cyt *c*; ESI-MS spectra of the purified I81N *h*Cyt *c*; UV−vis spectra of I81N and WT *h*Cyt *c*; CD spectra of the ferric WT and I81N *h*Cyt *c*; alkaline conformational transition of WT *h*Cyt *c*; acidic titration of WT *h*Cyt *c*; azide-binding experiment for WT *h*Cyt *c*; stopped-flow spectra of guaiacol oxidation by H_2O_2 catalyzed by WT or I81N *h*Cyt *c*; Michaelis−Menten plots for WT *h*Cyt *c* at pH 5−8; time-dependent UV−vis spectra of WT *h*Cyt *c* in a reaction with H_2O_2; multisequence alignment of vertebrate Ngb; 20 lowest energy solution structures of the reduced (PDB code 2N9I) and oxidized (PDB code 2N9J) *h*Cyt *c* solved by NMR; cryo-EM structure of the apoptosome complex (PDB codes 3JBT and 5JUY); representative ITC thermogram of WT *h*Cyt *c* titrated into *h*Ngb; and rmsd of the Cα atoms in a 200 ns molecular dynamics simulation trajectory (PDF)

■ AUTHOR INFORMATION

Corresponding Author

Ying-Wu Lin − *School of Chemistry and Chemical Engineering, University of South China, Hengyang 421001, China; Key Lab of Protein Structure and Function of Universities in Hunan Province, University of South China, Hengyang 421001, China;* orcid.org/0000-0002-2457-0871; Phone: (+86)734-8282375; Email: ywlin@usc.edu.cn

Authors

Yu Feng − *School of Chemistry and Chemical Engineering, University of South China, Hengyang 421001, China*

Xi-Chun Liu − *School of Chemistry and Chemical Engineering, University of South China, Hengyang 421001, China*

Lianzhi Li − *School of Chemistry and Chemical Engineering, Liaocheng University, Liaocheng 252059, China;* orcid.org/0000-0002-8447-3803

Shu-Qin Gao − *Key Lab of Protein Structure and Function of Universities in Hunan Province, University of South China, Hengyang 421001, China*

Ge-Bo Wen − *Key Lab of Protein Structure and Function of Universities in Hunan Province, University of South China, Hengyang 421001, China*

Complete contact information is available at: https://pubs.acs.org/10.1021/acsomega.2c01256

Author Contributions

‖Y.F. and X.-C.L. contributed equally.

Notes

The authors declare no competing financial interest.

■ ACKNOWLEDGMENTS

We gratefully thank Prof. T. Burmester of the Gutenberg University of Mainz, Germany, for graciously providing the gene of human Ngb. The pBTR1 plasmid containing the coding sequence of the WT *h*cyt *c* gene was obtained from Addgene (no. 22468). This work was supported by the National Natural Science Foundation of China (21977042 and 32171270).

■ REFERENCES

(1) Bertini, I.; Cavallaro, G.; Rosato, A. Cytochrome c: occurrence and functions. *Chem. Rev.* **2006**, *106*, 90−115.

(2) Smith, L. J.; Kahraman, A.; Thornton, J. M. Heme proteins–diversity in structural characteristics, function, and folding. *Proteins* **2010**, *78*, 2349−2368.

(3) Liu, J.; Chakraborty, S.; Hosseinzadeh, P.; Yu, Y.; Tian, S.; Petrik, I.; Bhagi, A.; Lu, Y. Metalloproteins Containing Cytochrome, Iron−Sulfur, or Copper Redox Centers. *Chem. Rev.* **2014**, *114*, 4366−4469.

(4) Hannibal, L.; Tomasina, F.; Capdevila, D. A.; Demicheli, V.; Tórtora, V.; Alvarez-Paggi, D.; Jemmerson, R.; Murgida, D. H.; Radi, R. Alternative Conformations of Cytochrome c: Structure, Function, and Detection. *Biochemistry* **2016**, *55*, 407−428.

(5) Alvarez-Paggi, D.; Hannibal, L.; Castro, M. A.; Oviedo-Rouco, S.; Demicheli, V.; Tórtora, V.; Tomasina, F.; Radi, R.; Murgida, D. H. Multifunctional Cytochrome c: Learning New Tricks from an Old Dog. *Chem. Rev.* **2017**, *117*, 13382−13460.

(6) Lin, Y.-W. Structure and function of heme proteins regulated by diverse post-translational modifications. *Arch. Biochem. Biophys.* **2018**, *641*, 1−30.

(7) Rajagopal, B. S.; Edzuma, A. N.; Hough, M. A.; Blundell, K. L. I. M.; Kagan, V. E.; Kapralov, A. A.; Fraser, L. A.; Butt, J. N.; Silkstone, G. G.; Wilson, M. T.; et al. The hydrogen-peroxide-induced radical behaviour in human cytochrome c-phospholipid complexes: implications for the enhanced pro-apoptotic activity of the G41S mutant. *Biochem. J.* **2013**, *456*, 441−452.

(8) Santucci, R.; Sinibaldi, F.; Cozza, P.; Polticelli, F.; Fiorucci, L. Cytochrome c: An extreme multifunctional protein with a key role in cell fate. *Int. J. Biol. Macromol.* **2019**, *136*, 1237−1246.

(9) McClelland, L. J.; Mou, T.-C.; Jeakins-Cooley, M. E.; Sprang, S. R.; Bowler, B. E. Structure of a mitochondrial cytochrome c conformer competent for peroxidase activity. *Proc. Natl. Acad. Sci. U.S.A.* **2014**, *111*, 6648−6653.

(10) Matsuyama, S.; Llopis, J.; Deveraux, Q. L.; Tsien, R. Y.; Reed, J. C. Changes in intramitochondrial and cytosolic pH: early events that modulate caspase activation during apoptosis. *Nat. Cell Biol.* **2000**, *2*, 318−325.

(11) Bandi, S.; Bowler, B. E. Effect of an Ala81His mutation on the Met80 loop dynamics of iso-1-cytochrome c. *Biochemistry* **2015**, *54*, 1729−1742.

(12) Wang, Z.-H.; Lin, Y.-W.; Rosell, F. I.; Ni, F.-Y.; Lu, H.-J.; Yang, P.-Y.; Tan, X.-S.; Li, X.-Y.; Huang, Z.-X.; Mauk, A. G. Converting cytochrome c into a peroxidase-like metalloenzyme by molecular design. *Chembiochem* **2007**, *8*, 607−609.

(13) Wang, Z.; Matsuo, T.; Nagao, S.; Hirota, S. Peroxidase activity enhancement of horse cytochrome c by dimerization. *Org. Biomol. Chem.* **2011**, *9*, 4766−4769.
(14) Wang, Z.; Ando, Y.; Nugraheni, A. D.; Ren, C.; Nagao, S.; Hirota, S. Self-oxidation of cytochrome c at methionine80 with molecular oxygen induced by cleavage of the Met-heme iron bond. *Mol. Biosyst.* **2014**, *10*, 3130−3137.
(15) Nugraheni, A. D.; Ren, C.; Matsumoto, Y.; Nagao, S.; Yamanaka, M.; Hirota, S. Oxidative modification of methionine80 in cytochrome c by reaction with peroxides. *J. Inorg. Biochem.* **2018**, *182*, 200−207.
(16) Ying, T.; Wang, Z.-H.; Lin, Y.-W.; Xie, J.; Tan, X.; Huang, Z.-X. Tyrosine-67 in cytochrome c is a possible apoptotic trigger controlled by hydrogen bonds via a conformational transition. *Chem. Commun.* **2009**, 4512−4514.
(17) Lan, W.; Wang, Z.; Yang, Z.; Ying, T.; Zhang, X.; Tan, X.; Liu, M.; Cao, C.; Huang, Z.-X. Structural basis for cytochrome c Y67H mutant to function as a peroxidase. *PLoS One* **2014**, *9*, No. e107305.
(18) Lou, D.; Liu, X.-C.; Wang, X.-J.; Gao, S.-Q.; Wen, G.-B.; Lin, Y.-W. The importance of Asn52 in the structure−function relationship of human cytochrome c. *RSC Adv.* **2020**, *10*, 44768−44772.
(19) Nold, S. M.; Lei, H.; Mou, T.-C.; Bowler, B. E. Effect of a K72A Mutation on the Structure, Stability, Dynamics, and Peroxidase Activity of Human Cytochrome c. *Biochemistry* **2017**, *56*, 3358−3368.
(20) McClelland, L. J.; Steele, H. B. B.; Whitby, F. G.; Mou, T.-C.; Holley, D.; Ross, J. B. A.; Sprang, S. R.; Bowler, B. E. Cytochrome c Can Form a Well-Defined Binding Pocket for Hydrocarbons. *J. Am. Chem. Soc.* **2016**, *138*, 16770−16778.
(21) Mandal, A.; Hoop, C. L.; DeLucia, M.; Kodali, R.; Kagan, V. E.; Ahn, J.; van der Wel, P. C. A. Structural Changes and Proapoptotic Peroxidase Activity of Cardiolipin-Bound Mitochondrial Cytochrome c. *Biophys. J.* **2015**, *109*, 1873−1884.
(22) Parui, P. P.; Sarakar, Y.; Majumder, R.; Das, S.; Yang, H.; Yasuhara, K.; Hirota, S. Determination of proton concentration at cardiolipin-containing membrane interfaces and its relation with the peroxidase activity of cytochrome c. *Chem. Sci.* **2019**, *10*, 9140−9151.
(23) Burmester, T.; Weich, B.; Reinhardt, S.; Hankeln, T. A vertebrate globin expressed in the brain. *Nature* **2000**, *407*, 520−523.
(24) Fago, A.; Mathews, A. J.; Moens, L.; Dewilde, S.; Brittain, T. The reaction of neuroglobin with potential redox protein partners cytochrome b5 and cytochrome c. *FEBS Lett.* **2006**, *580*, 4884−4888.
(25) Basu, S.; Keszler, A.; Azarova, N. A.; Nwanze, N.; Perlegas, A.; Shiva, S.; Broniowska, K. A.; Hogg, N.; Kim-Shapiro, D. B. A novel role for cytochrome c: Efficient catalysis of S-nitrosothiol formation. *Free Radic. Biol. Med.* **2010**, *48*, 255−263.
(26) Tiwari, P. B.; Chapagain, P. P.; Üren, A. Investigating molecular interactions between oxidized neuroglobin and cytochrome c. *Sci. Rep.* **2018**, *8*, 10557.
(27) Lek, M.; Karczewski, K. J.; Minikel, E. V.; Samocha, K. E.; Banks, E.; Fennell, T.; O'Donnell-Luria, A. H.; Ware, J. S.; Hill, A. J.; et al. Analysis of protein-coding genetic variation in 60,706 humans. *Nature* **2016**, *536*, 285−291.
(28) Karsisiotis, A. I.; Deacon, O. M.; Wilson, M. T.; Macdonald, C.; Blumenschein, T. M. A.; Moore, G. R.; Worrall, J. A. R. Increased dynamics in the 40-57 Omega-loop of the G41S variant of human cytochrome c promote its pro-apoptotic conformation. *Sci. Rep.* **2016**, *6*, 30447.
(29) Deacon, O. M.; Svistunenko, D. A.; Moore, G. R.; Wilson, M. T.; Worrall, J. A. R. Naturally Occurring Disease-Related Mutations in the 40-57 Omega-Loop of Human Cytochrome c Control Triggering of the Alkaline Isomerization. *Biochemistry* **2018**, *57*, 4276−4288.
(30) Lei, H.; Bowler, B. E. Naturally Occurring A51V Variant of Human Cytochrome c Destabilizes the Native State and Enhances Peroxidase Activity. *J. Phys. Chem. B* **2019**, *123*, 8939−8953.
(31) Deacon, O. M.; White, R. W.; Moore, G. R.; Wilson, M. T.; Worrall, J. A. R. Comparison of the structural dynamic and mitochondrial electron-transfer properties of the proapoptotic human cytochrome c variants, G41S, Y48H and A51V. *J. Inorg. Biochem.* **2020**, *203*, 110924.
(32) Lei, H.; Nold, S. M.; Motta, L. J.; Bowler, B. E. Effect of V83G and I81A Substitutions to Human Cytochrome c on Acid Unfolding and Peroxidase Activity below a Neutral pH. *Biochemistry* **2019**, *58*, 2921−2933.
(33) Jumper, J.; Evans, R.; Pritzel, A.; Green, T.; Figurnov, M.; Ronneberger, O.; Tunyasuvunakool, K.; Bates, R.; Žídek, A.; Potapenko, A.; et al. Highly accurate protein structure prediction with AlphaFold. *Nature* **2021**, *596*, 583−589.
(34) Evans, R.; O'Neill, M.; Pritzel, A.; Antropova, N.; Senior, A.; Green, T.; Žídek, A.; Bates, R.; Blackwell, S.; Yim, J.; Ronneberger, O.; Bodenstein, S.; Zielinski, M.; Bridgland, A.; Potapenko, A.; Cowie, A.; Tunyasuvunakool, K.; Jain, R.; Clancy, E.; Kohli, P.; Jumper, J.; Hassabis, D. Protein complex prediction with AlphaFold-Multimer. **2021**, Biorxiv: 10.1101/2021.10.04.463034.
(35) Perez-Iratxeta, C.; Andrade-Navarro, M. A. K2D2: estimation of protein secondary structure from circular dichroism spectra. *BMC Struct. Biol.* **2008**, *8*, 25.
(36) Theorell, H.; Åkesson, Å. Studies on cytochrome c. III. Titration curves. *J. Am. Chem. Soc.* **1941**, *63*, 1818−1820.
(37) Rosell, F. I.; Ferrer, J. C.; Mauk, A. G. Proton-linked protein conformational switching: Definition of the alkaline conformational transition of yeast iso-1-ferricytochrome c. *J. Am. Chem. Soc.* **1998**, *120*, 11234−11245.
(38) Nilsson, C.; Kågedal, K.; Johansson, U.; Öllinger, K. Analysis of cytosolic and lysosomal pH in apoptotic cells by flow cytometry. *Methods Cell Sci.* **2004**, *25*, 185−194.
(39) Rosell, F. I.; Harris, T. R.; Hildebrand, D. P.; Döpner, S.; Hildebrandt, P.; Mauk, A. G. Characterization of an alkaline transition intermediate stabilized in the Phe82Trp variant of yeast iso-1-cytochrome c. *J. Biochem.* **2000**, *39*, 9047−9054.
(40) Lalli, D.; Rosa, C.; Allegrozzi, M.; Turano, P. Distal Unfolding of Ferricytochrome c Induced by the F82K Mutation. *Int. J. Mol. Sci.* **2020**, *21*, 2134.
(41) Samsri, S.; Prasertsuk, P.; Nutho, B.; Pornsuwan, S. Molecular insights on the conformational dynamics of a P76C mutant of human cytochrome c and the enhancement on its peroxidase activity. *Arch. Biochem. Biophys.* **2022**, *716*, 109112.
(42) Zhong, F.; Alden, S. L.; Hughes, R. P.; Pletneva, E. V. Comparing Properties of Common Bioinorganic Ligands with Switchable Variants of Cytochrome c. *Inorg. Chem.* **2022**, *61*, 1207−1227.
(43) Samsri, S.; Pornsuwan, S. Influence of cysteine-directed mutations at the Omega-loops on peroxidase activity of human cytochrome c. *Arch. Biochem. Biophys.* **2021**, *709*, 108980.
(44) Porcelli, A. M.; Ghelli, A.; Zanna, C.; Pinton, P.; Rizzuto, R.; Rugolo, M. pH difference across the outer mitochondrial membrane measured with a green fluorescent protein mutant. *Biochem. Biophys. Res. Commun.* **2005**, *326*, 799−804.
(45) Matsui, T.; Nakajima, A.; Fujii, H.; Matera, K. M.; Migita, C. T.; Yoshida, T.; Ikeda-Saito, M. O_2-and H_2O_2-dependent verdoheme degradation by heme oxygenase: Reaction mechanisms and potential physiological roles of the dual pathway degradation. *Biol. Chem.* **2005**, *280*, 36833−36840.
(46) Tomášková, N.; Varinska, L.; Sedlak, E. Rate of oxidative modification of cytochrome c by hydrogen peroxide is modulated by Hofmeister anions. *Gen. Physiol. Biophys.* **2010**, *29*, 255−265.
(47) Auer, M.; Nicolussi, A.; Schütz, G.; Furtmüller, P. G.; Obinger, C. How covalent heme to protein bonds influence the formation and reactivity of redox intermediates of a bacterial peroxidase. *J. Biol. Chem.* **2014**, *289*, 31480−31491.
(48) Yan, D.-J.; Yuan, H.; Li, W.; Xiang, Y.; He, B.; Nie, C.-M.; Wen, G.-B.; Lin, Y.-W.; Tan, X. How a novel tyrosine-heme cross-link fine-tunes the structure and functions of heme proteins: a direct comparitive study of L29H/F43Y myoglobin. *Dalton Trans.* **2015**, *44*, 18815−18822.
(49) Tiwari, P. B.; Astudillo, L.; Pham, K.; Wang, X.; He, J.; Bernad, S.; Derrien, V.; Sebban, P.; Miksovska, J.; Darici, Y. Characterization of molecular mechanism of neuroglobin binding to cytochrome c: A

https://doi.org/10.1021/acsomega.2c01256
ACS Omega 2022, 7, 11510−11518

surface plasmon resonance and isothermal titration calorimetry study. *Inorg. Chem. Commun.* **2015**, *62*, 37−41.
(50) Bønding, S. H.; Henty, K.; Dingley, A. J.; Brittain, T. The binding of cytochrome c to neuroglobin: a docking and surface plasmon resonance study. *Int. J. Biol. Macromol.* **2008**, *43*, 295−299.
(51) Tejero, J. Negative surface charges in neuroglobin modulate the interaction with cytochrome c. *Biochem. Biophys. Res. Commun.* **2020**, *523*, 567−572.
(52) Yu, T.; Wang, X.; Purring-Koch, C.; Wei, Y.; McLendon, G. L. A mutational epitope for cytochrome C binding to the apoptosis protease activation factor-1. *J. Biol. Chem.* **2001**, *276*, 13034−13038.

https://doi.org/10.1021/acsomega.2c01256
ACS Omega 2022, 7, 11510−11518